

A Marching Procedure for Form-finding for Tensegrity Structures

A. Micheletti

*Dipartimento di Ingegneria Civile
Università di Roma “Tor Vergata”
Via Politecnico 1, 00133 Roma, Italy*

W. O. Williams

*Department of Mathematical Sciences
Carnegie Mellon University
Pittsburgh, PA 15213-3890 USA*

Abstract

The problem of form-finding for a tensegrity structure is considered. We describe a method of arriving at stable placements of a given tensegrity structure by starting from a known stable placement and altering edge-lengths in a way consistent with the restrictions of the equilibrium equations. As an introduction, the main previous results concerning stability are presented. Deeper insight in the form-finding process is then offered through the characterization of the manifold to which classical tensegrity systems belong. Several special cases are illustrated. A final example of a large system shows the reliability of the method.

Key words: Tensegrity structures, stability analysis, rank-deficiency manifold, marching processes, limit placements

1 Introduction

Tensegrity structures, popularized by Buckminster Fuller following sculptures by Kenneth Snelson, have become familiar to most structural engineers and

Email addresses: micheletti@ing.uniroma2.it (A. Micheletti), wow@cmu.edu (W. O. Williams).

architects through their applications, in particular, to lightweight domes (Pellegrino (1992) [37]) and to decorative structures (Snelson (1996) [43]). These structures consist in a combination of rigid bars, which carry tension or compression, and inextensible cables, which can carry no compression, with elements connected at their ends by pin joints.¹

The analysis of the kinematics and mechanics of such structures has roots in the engineering studies of trusses done by Möbius (1837) [26] and Maxwell (1869) [23] and in the mathematical studies by Cauchy (1813) [9] of the rigidity of polygonal frames. These early studies considered only traditional pinned-bar structures. Extension of the concepts to tensegrity structures originated with Calladine (1978) [7], Pellegrino *et al.* (1986) [36] and Calladine *et al.* (1991) [8] in the engineering literature, and with Roth *et al.* (1981) [39] in mathematical literature. Extensive bibliographies and more recent results appear in Connelly *et al.* (1996) [10], Skelton *et al.* (2001) [44], Motro (2003) [28], Tibert *et al.* (2003) [51], Masic *et al.* (2006) [22], So *et al.* (2006) [46]; *cf* Williams (2003) [54].

Our interest here is in the “form-finding problem”: given the “topology”, *ie*, the diagram of the connection pattern (the graph) of the structure, along with a description of the relative positions of crossing elements if the graph is not planar, one seeks to find which physical placements in space will result in a stable structure.

Several different methods have been used to attack the form-finding problem, *cf* Tibert *et al.* (2003) [51]. Motro (1984) [27] employed the method of dynamic relaxation, a technique first introduced by Day (1965) [12] that is reliably applied to tensile structures, *eg*, Barnes (1999) [5], and to many other non-linear problems. Pellegrino (1986) [35] formulated an equivalent constrained minimization problem and, since 1994, the techniques of non-linear programming have been extensively used by Burkhardt (2005) [6]. Connelly *et al.* (1998) [11] applied group representation theory to discover numerous symmetric placements. Vassart *et al.* (1999) [52] employed the force density method, first introduced by Linkwitz *et al.* (1971) [21] (Schek (1974) [41]) for form-finding of tensile structures. Skelton *et al.* (2002) [45] presented an algebraic approach specialized to structures with non-contiguous bars. Recently, genetic algorithms has been employed by Paul *et al.* (2005) [33]. Lastly, Zhang *et al.* (2005) [55] and Gomez Estrada *et al.* (2006) [18] presented new numerical methods using a force density formulation, while Zhang *et al.* (2006) [56] employed a refined dynamic relaxation procedure.

This problem has no complete solution, although many authors have examined

¹ Without essential change in the computations, one may also introduce elements which are unpinned bars which may admit no tension. These conventionally are called struts; since they are of less practical interest, we choose not to include them.

sufficient conditions. The most convenient sufficient condition, which we use here, is the second-order stress test. This test is stronger than the condition of minimality of energy, but equivalent to it in most common situations. More precisely, it is not a necessary condition for stability, since there can be stable structures for which it is not satisfied, but it is a necessary and sufficient condition in order to have a structure possessing first-order positive stiffness. Note that we model bars as rigid and cable as inextensible, therefore, local or global buckling instabilities, depending on the material properties of the elements in a physical structure, must be considered separately (*cf* Ohsaki *et al.* (2005) [31]).

Unfortunately, the known stability conditions, including the second-order test, are descriptive rather than prescriptive. That is, they are tests easily applied to a given placement of the structure, but are difficult to exploit, even numerically, to discover stable placements. We propose a practical method of attacking the form-finding problem which is based on setting up a system of differential equations which can be solved (numerically) to obtain a family of stable placements. The trajectory of these solutions must initiate at a stable placement, so the process requires we have a beginning point which is a stable structure. However, there are many examples in the literature of such placements, most of whose (analytic) construction is enabled by a high degree of symmetry, *eg* Nishimura (2000) [30] (Murakami *et al.* (2001) [29]), Sultan *et al.* (2001) [48], Micheletti (2003) [24].

The method has practical relevance in all those applications where it is important to pass from one configuration to another by continuously controlling the lengths of the elements, *ie* for foldable/deployable or variable geometry structures. The analysis and design of tensegrity structures for this kind of applications as been pioneered by Furuya (1992) [16] and Hanaor (1993) [19], then continued with Oppenheim *et al.* (1997) [32], Bouderbala *et al.* (1998) [4], Sultan *et al.* (1998) [47]. More recent studies can be found in Tibert (2002) [50], Aldrich *et al.* (2003) [1], Defossez (2003) [13], El Smaili *et al.* (2004) [14], Fest *et al.* (2004) [15] Paul *et al.* (2005) [34], Schenk *et al.* (2006) [42].

In order to discuss the use, and the limitations, of the form-finding process, after introducing notation and concepts in Section 2, in Section 3 we present some general results about tensegrity structures, most of which appear in the published literature, but which are scattered through the mathematical and engineering literature. We also present several simple examples of structures to illustrate the limitations of the results. Section 4 is devoted to characterization of the sets of placements to which our method applies, the rank-deficient manifolds. We briefly illustrate singular cases within the characterization. We present a description of the details of our algorithm in Section 5, and give examples of its application.

2 Structural Analysis of Trusses

Engineering analysis of trusses (a two-dimensional² example of a truss appears in Figure 1), is convenient to carry out by use of the *structural* or *equilibrium matrix* \mathbf{A} . If \mathbf{f} denotes the vector consisting of the externally applied forces, indexed by nodes (pin-joints) of the structure and $\boldsymbol{\tau}$ the vector of forces in the edges (bars) of the structure, indexed by edge, then there is a linear relation between the two, as

$$\mathbf{f} = \mathbf{A}\boldsymbol{\tau}. \quad (1)$$

Dual to this is the relation between \mathbf{v} , the vector of velocities (or, in engineering terms, infinitesimal motions) of the nodes, and $\boldsymbol{\delta}$, the vector of rates of lengthening of the edges, as

$$\boldsymbol{\delta} = \mathbf{A}^T \mathbf{v}. \quad (2)$$

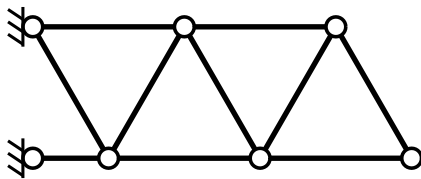


Fig. 1. A simple two-dimensional truss

We will consider a variation of this model which is more convenient for calculations. To make things precise, we consider a structure in three dimensions, with n pins, or **nodes**, located at the **placement**

$$\mathbb{p} := (\mathbf{p}_1, \dots, \mathbf{p}_n); \quad \mathbf{p}_r \in \mathbb{R}^3 \quad (3)$$

Then the collection of members of the structure, the **edges**, is labeled by giving the end-nodes of each edge, as

$$\mathcal{E} := \{ \{ij\} \}. \quad (4)$$

We suppose there are k edges. Next, we construct a matrix $\mathbf{\Pi}$ by specifying

² All of our examples will be two dimensional, to avoid over-complicated diagrams.

its column vectors, one per edge, as

$$\boldsymbol{\pi}_{ij}(\mathbb{P}) = \begin{bmatrix} \mathbf{0} \\ \vdots \\ \mathbf{0} \\ \mathbf{p}_i - \mathbf{p}_j \\ \mathbf{0} \\ \vdots \\ \mathbf{0} \\ \mathbf{p}_j - \mathbf{p}_i \\ \mathbf{0} \\ \vdots \\ \mathbf{0} \end{bmatrix} \in \mathbb{R}^{3n}. \quad (5)$$

Here the entries, indexed by the list of nodes, are values in \mathbb{R}^3 ; the non-zero entries in (5) are in the i th and j th rows, respectively. The matrix Π , conventionally used in the geometry literature, we call the **geometric matrix**. To change this matrix into the corresponding equilibrium matrix \mathbf{A} , one divides each column vector $\boldsymbol{\pi}_{ij}$ by the length of the corresponding edge.

With this formulation and with the force vector of external forces applied to the nodes, denoted \mathfrak{f} as before, balance of forces at each node is expressed as

$$\mathfrak{f} = \Pi \boldsymbol{\omega}, \quad (6)$$

where $\boldsymbol{\omega}$ is a vector in \mathbb{R}^k whose ij entry is *the scalar force in the edge ij divided by the length of the edge*. We will refer to $\boldsymbol{\omega}$ as the **stress** vector for the placement³. Physically, one pictures an applied set of nodal forces generating stresses in the structure to support them. If the structure is redundant (“excess” number of edges) it may admit a self-equilibrating stress or **self stress** $\boldsymbol{\omega}$ satisfying

$$\Pi \boldsymbol{\omega} = \mathbf{0}. \quad (7)$$

Next, we turn to kinematics. We consider a velocity (*alt*, infinitesimal motion) \mathfrak{v} , as before. Then Π associates to \mathfrak{v} a rate of lengthening in each edge of the structure via

$$\boldsymbol{\epsilon} = \Pi^T \mathfrak{v} \quad (8)$$

³ Often, in the literature, ω_{ij} is referred to as the *force density* of the element ij .

or

$$\epsilon_{ij} = \boldsymbol{\pi}_{ij} \cdot \mathbf{v} = (\mathbf{p}_i - \mathbf{p}_j) \cdot (\mathbf{v}_i - \mathbf{v}_j). \quad (9)$$

ϵ_{ij} is the rate of lengthening of edge ij times the length of the edge. Physically, we picture a velocity imposed on each node generating lengthening or shortening of the edges.

We choose to consider only *constrained* structures, with several nodes fixed to earth. These nodes can admit only zero velocities, and we consider only cases in which enough are fixed that there can be no rigid-body motions of the entire structure.⁴ For such a structure, a velocity which leaves all edge-lengths unchanged must represent a flexibility in the structure. If $\mathbf{v} \neq \mathbf{0}$ and

$$\boldsymbol{\Pi}^\top \mathbf{v} = \mathbf{0}. \quad (10)$$

we call \mathbf{v} a flexure or a **mechanism**.

The set of all self stresses, the null space of $\boldsymbol{\Pi}$, is a subspace of \mathbb{R}^k ; we call its dimension, s , the *number* of self stresses. Likewise, if the null space of $\boldsymbol{\Pi}^\top$, whose non-zero elements are mechanisms, has dimension m , we call this the *number* of mechanisms.

Finally, we discuss stability. A **motion** of a structure is a time-parameterized family of placements, $\mathbf{q}(t)$; the time-derivative at 0, $\dot{\mathbf{q}}(0)$, is a velocity for the placement $\mathfrak{p} = \mathbf{q}(0)$. Since rigid-body motions are ruled out by our assumed constraints, an **admissible** motion of the structure, one which leaves edge-lengths unchanged, represents a mode of collapse of the structure. The initial velocity of a collapsing motion is a mechanism, but, in general, the existence of a mechanism does not ensure that there can be continuation to a collapsing motion. However, one can avoid collapsing by ensuring that no mechanisms can occur.

Our nomenclature reflects the distinction of these two possibilities: a placement of the structure is said to be **stable** if it admits no admissible motions away from that placement, and the structure is said to be **rigid** in that placement if it admits no mechanisms.⁵ Thus rigidity implies stability, but the converse is false, in general. (Asimow *et al.* (1979) [3], show that the converse

⁴ When a node is fixed to earth the corresponding entry in \mathfrak{p} carries a fixed value; in computations we may choose to reduce the size of the matrix $\boldsymbol{\Pi}$ by omitting rows which correspond to such fixed nodes. Likewise, we may remove any “edge” which consists of two fixed nodes.

⁵ Unfortunately, in the geometry literature what we call stability is called rigidity and what we call rigidity, is termed first-order rigidity. Our usage is closer to standard engineering nomenclature.

is true if the present placement produces a local maximum in rank for the geometric matrix.)

3 Tensegrity Structures

Tensegrity structures operate under a more restrictive set of rules.

First, note that the stress in an edge which is to be a cable must be non-negative (a tension). A stress vector ω which assigns a zero or positive tension to each cable we call **proper**; if it assigns a positive tension to each cable, we call it **strict**.

Second, we must broaden the definition of **admissible motion** to include those which, while keeping all bars at their initial length and cables unlengthened, may allow some cables to shorten.

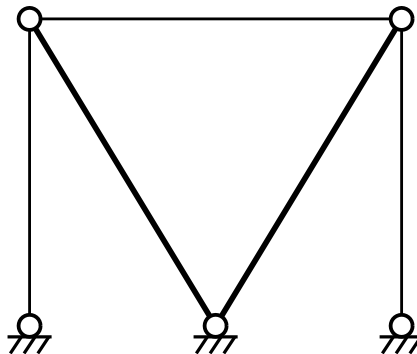


Fig. 2. A two-dimensional tensegrity structure

Correspondingly, the set of **admissible velocities** for a tensegrity structure will include not only all mechanisms but also all velocities v which satisfy

$$\pi_{ij} \cdot v \leq 0 \quad (11)$$

for all cables as well as $\pi_{ij} \cdot v = 0$ for all bars.

3.1 Expanded Kinematics and Kinematic Criteria for Stability

To formulate the stability conditions which we employ, we must consider motions in more detail. If a motion away from a placement of the structure can occur, we can calculate not only an initial velocity v , but also a series of higher-order coefficients.⁶ We follow Alexandrov (2001) [2], *cf* Williams (2003) [54], Connelly *et al.* (1996) [10], in calculation of the measure of the lengths of edges in a motion. Such computations, for bar structures, date back to Koiter (1984) [20] and Tarnai (1984) [49], who considered the question of higher-order mechanisms. See also the development in terms of elastic energies by Salerno

⁶ It can be shown that any motion which occurs may be supposed to be real analytic: see Glück (1975) [17].

(1992) [40], and the expansions similar to those below by Vassart *et al.* (2000) [53].

To formulate the length measure in a convenient way, note that from (5) we can see that the edge vector $\boldsymbol{\pi}_{ij}$ (column vector of $\boldsymbol{\Pi}$) is a linear function of the placement vector \mathfrak{p} . We formalize this as

$$\boldsymbol{\pi}_{ij}(\mathfrak{p}) = B_{ij}\mathfrak{p}. \quad (12)$$

It is easy to see that each operator B_{ij} is symmetric. The quantity

$$\lambda_{ij} = B_{ij}\mathfrak{p} \cdot \mathfrak{p} = \|\mathbf{p}_i - \mathbf{p}_j\|^2 \quad (13)$$

represents the squared length of the edge ij .

Let a motion from \mathfrak{p} be written as an expansion

$$\mathfrak{q}(t) = \sum_{n=0}^{\infty} t^n \mathfrak{q}_n \quad (14)$$

with coefficients \mathfrak{q}_n and with $\mathfrak{q}_0 = \mathfrak{p}$. For each edge ij , we calculate

$$\lambda_{ij}(t) = B_{ij} \left(\sum_{r=0}^{\infty} t^r \mathfrak{q}_r \right) \cdot \left(\sum_{p=0}^{\infty} t^p \mathfrak{q}_p \right) = \sum_{r,p=0}^{\infty} t^{r+p} B_{ij} \mathfrak{q}_r \cdot \mathfrak{q}_p. \quad (15)$$

Let $n = r + p$, we have $p = n - r \geq 0$, $r \leq n$, the previous expression becomes:

$$\sum_{r,p=0}^{\infty} t^{r+p} B_{ij} \mathfrak{q}_r \cdot \mathfrak{q}_p = \sum_{n=0}^{\infty} \left(\sum_{r=0}^n B_{ij} \mathfrak{q}_r \cdot \mathfrak{q}_{n-r} \right) t^n. \quad (16)$$

For $n = 0$, the first term of the sum is $B_{ij} \mathfrak{q}_0 \cdot \mathfrak{q}_0 = \lambda_{ij}(\mathfrak{p})$ and we have

$$\lambda_{ij}(t) = \lambda_{ij}(\mathfrak{p}) + \sum_{n=1}^{\infty} \left(\sum_{r=0}^n B_{ij} \mathfrak{q}_r \cdot \mathfrak{q}_{n-r} \right) t^n. \quad (17)$$

First, consider a bar. To be admissible the motion must ensure $\dot{\lambda}_{ij} = 0$, or

$$\sum_{r=0}^n B_{ij} \mathfrak{q}_r \cdot \mathfrak{q}_{n-r} = 0 \quad n = 1, 2, \dots, \quad (18)$$

and, since $B_{ij} \mathfrak{q}_0 = \boldsymbol{\pi}_{ij}$ and B_{ij} is symmetric, we have the **recursion relation**

$$2\boldsymbol{\pi}_{ij} \cdot \mathfrak{q}_n = - \sum_{r=1}^{n-1} B_{ij} \mathfrak{q}_r \cdot \mathfrak{q}_{n-r} \quad n = 1, 2, \dots \quad (19)$$

For reference, the first few terms are

$$\begin{aligned}
2 \boldsymbol{\pi}_{ij} \cdot \mathbf{q}_1 &= 0 \\
2 \boldsymbol{\pi}_{ij} \cdot \mathbf{q}_2 &= -B_{ij} \mathbf{q}_1 \cdot \mathbf{q}_1 \\
2 \boldsymbol{\pi}_{ij} \cdot \mathbf{q}_3 &= -2 B_{ij} \mathbf{q}_2 \cdot \mathbf{q}_1 \\
2 \boldsymbol{\pi}_{ij} \cdot \mathbf{q}_4 &= -2 B_{ij} \mathbf{q}_1 \cdot \mathbf{q}_3 - B_{ij} \mathbf{q}_2 \cdot \mathbf{q}_2.
\end{aligned} \tag{20}$$

Recall that we are abbreviating $\boldsymbol{\pi}_{ij} = \boldsymbol{\pi}_{ij}(\mathbb{P})$. The conditions could also be written in the shorter form

$$\begin{aligned}
2 \boldsymbol{\pi}_{ij} \cdot \mathbf{q}_1 &= 0 \\
2 \boldsymbol{\pi}_{ij} \cdot \mathbf{q}_2 &= -\boldsymbol{\pi}_{ij}(\mathbf{q}_1) \cdot \mathbf{q}_1 \\
&\text{etc.}
\end{aligned}$$

and, if *all* edges are unchanged in length, as

$$\begin{aligned}
2 \Pi^\top \mathbf{q}_1 &= 0 \\
2 \Pi^\top \mathbf{q}_2 &= -\Pi(\mathbf{q}_1)^\top \cdot \mathbf{q}_1 \\
&\text{etc.}
\end{aligned} \tag{21}$$

This formalism will be useful below.

For a cable the recursion is similar, but may truncate. The conditions are

$$\sum_{r=0}^n B_{ij} \mathbf{q}_r \cdot \mathbf{q}_{n-r} \leq 0 \quad n = 1, 2, \dots, \tag{22}$$

yielding the recursion

$$2 \boldsymbol{\pi}_{ij} \cdot \mathbf{q}_n \leq -\sum_{r=1}^{n-1} B_{ij} \mathbf{q}_r \cdot \mathbf{q}_{n-r} \quad n = 1, 2, \dots, \tag{23}$$

with the understanding that the recursion truncates at the first n for which inequality obtains.

Thus the algorithm for a cable is:

1. If for a cable $2 \boldsymbol{\pi}_{ij} \cdot \mathbf{q}_1 < 0$, then the motion is admissible for that component with no further testing needed.
 2. If for a cable $2 \boldsymbol{\pi}_{ij} \cdot \mathbf{q}_1 = 0$ but $2 \boldsymbol{\pi}_{ij} \cdot \mathbf{q}_2 < -B_{ij} \mathbf{q}_1 \cdot \mathbf{q}_1$, then the motion is admissible for that component with no further testing needed.
 3. If for a cable $2 \boldsymbol{\pi}_{ij} \cdot \mathbf{q}_1 = 0$ and $2 \boldsymbol{\pi}_{ij} \cdot \mathbf{q}_2 = -B_{ij} \mathbf{q}_1 \cdot \mathbf{q}_1$ but $2 \boldsymbol{\pi}_{ij} \cdot \mathbf{q}_3 < -2 B_{ij} \mathbf{q}_2 \cdot \mathbf{q}_1$, then the motion is admissible for that component with no further testing needed.
- etc.

The simplest way to ensure stability is to rule out expansions of the sort outlined above. Note that the $n = 1$ case from each of (18) and (23) combine to require that \mathfrak{q}_1 is an admissible velocity. But, moreover, if all coefficients in the expansion (14) are zero up to the p -th, then \mathfrak{q}_p satisfies the condition to be an admissible velocity. We denote the first non-zero coefficient as $\mathfrak{v} = \mathfrak{q}_p$ and the next two coefficient in the expansion as $\mathfrak{a} = \mathfrak{q}_{p+1}$, $\mathfrak{j} = \mathfrak{q}_{p+2}$. Hence, as we have noted,

Criterion 1 (Kinematic Test 1) *If there is no non-zero admissible velocity \mathfrak{v} for a placement then the structure is stable in that placement.*

The second-order test of Connelly and Whiteley occurs at the next step. if the first non-zero coefficient in the expansion is \mathfrak{v} , the next term \mathfrak{a} must satisfy, if $\boldsymbol{\pi}_{ij} \cdot \mathfrak{v} = 0$,

$$2 \boldsymbol{\pi}_{ij} \cdot \mathfrak{a} \leq -B_{ij} \mathfrak{v} \cdot \mathfrak{v}, \quad (24)$$

with equality required if the edge is a bar. If, for a cable, $\boldsymbol{\pi}_{ij} \cdot \mathfrak{v} < 0$, then there is no second-order requirement. Formally, then

Criterion 2 (Kinematic Test 2) *Given a placement, if for any admissible velocity \mathfrak{v} there is no admissible acceleration, ie, no \mathfrak{a} such that*

$$2 \boldsymbol{\pi}_{ij} \cdot \mathfrak{a} = -B_{ij} \mathfrak{v} \cdot \mathfrak{v}, \text{ for each bar} \quad (25)$$

and, for each cable for which $\boldsymbol{\pi}_{ij} \cdot \mathfrak{v} = 0$,

$$2 \boldsymbol{\pi}_{ij} \cdot \mathfrak{a} \leq -B_{ij} \mathfrak{v} \cdot \mathfrak{v} \quad (26)$$

then the structure is stable in that placement.

The next test is similar. If the first two non-zero coefficients are admissible, then we look at the next:

Criterion 3 (Kinematic Test 3) *Given a placement, if for any admissible velocity \mathfrak{v} and acceleration \mathfrak{a} , there is no \mathfrak{j} such that*

$$2 \boldsymbol{\pi}_{ij} \cdot \mathfrak{j} = -2 B_{ij} \mathfrak{a} \cdot \mathfrak{v}, \text{ for each bar} \quad (27)$$

and, for each cable for which $\boldsymbol{\pi}_{ij} \cdot \mathfrak{v} = 0$ and $2 \boldsymbol{\pi}_{ij} \cdot \mathfrak{a} = -B_{ij} \mathfrak{v} \cdot \mathfrak{v}$ we have

$$2 \boldsymbol{\pi}_{ij} \cdot \mathfrak{j} \leq -2 B_{ij} \mathfrak{a} \cdot \mathfrak{v} \quad (28)$$

then the structure is stable in that placement.

It is straightforward to continue this to higher orders.

The more elaborate conditions of Alexandrov (2001) [2] for bar structures also can be extended to tensegrity structures.

3.2 Stress Tests

The direct tests of the last section are not easy to implement; here we discuss simpler tests.

First, let us consider the simplest form of a stress test. Given a placement \mathfrak{p} , suppose that there is a mechanism \mathfrak{v} , and we want to see whether there is a continued second-order term which conserves edge-lengths. Then (25) seeks a solution \mathfrak{a} to

$$2\Pi(\mathfrak{p})^\top \mathfrak{a} = -\Pi(\mathfrak{v})^\top \mathfrak{v}. \quad (29)$$

By a standard argument in linear algebra, there is a solution if and only if the right-hand side is perpendicular to all solutions of the homogeneous equation $\Pi(\mathfrak{p})\boldsymbol{\omega} = \mathbf{0}$. Thus (29) has a solution if and only if

$$\boldsymbol{\omega} \cdot \Pi(\mathfrak{v})^\top \mathfrak{v} = \Pi(\mathfrak{v})\boldsymbol{\omega} \cdot \mathfrak{v} = 0 \quad (30)$$

holds for all self stresses; if for some self stress this does not hold, the expansion of the motion cannot be continued beyond the first order.

The generalization of this result to tensegrity structures depends on an extension of the orthogonality test, relating convex sets rather than subspaces.

Proposition 4 *Given a placement and given $\boldsymbol{\epsilon} \in \mathbb{R}^k$ there exists a velocity \mathfrak{w} such that*

$$\boldsymbol{\pi}_{ij} \cdot \mathfrak{w} = \epsilon_{ij} \text{ for every bar,} \quad (31)$$

$$\boldsymbol{\pi}_{ij} \cdot \mathfrak{w} \leq \epsilon_{ij} \text{ for every cable,} \quad (32)$$

if and only if for every proper self stress $\boldsymbol{\omega}$

$$\boldsymbol{\omega} \cdot \boldsymbol{\epsilon} \geq 0. \quad (33)$$

A proof of this can be found in Williams (2003) [54], *cf* Connelly *et al.* (1996) [10].

A useful corollary of this is the **zero-self stress condition** due to Roth *et al.* (1981) [39]: there is an admissible velocity which shortens a particular cable if and only if all self stresses leave that cable unstressed.

From (33), replacing ϵ_{ij} by $-B_{ij} \mathfrak{v} \cdot \mathfrak{v}$ we deduce a criterion for continuing an expansion past the first term \mathfrak{v} , that

$$\boldsymbol{\omega} \cdot \Pi(\mathfrak{v})^\top \mathfrak{v} = \Pi(\mathfrak{v})\boldsymbol{\omega} \cdot \mathfrak{v} \leq 0 \quad (34)$$

for all self stresses $\boldsymbol{\omega}$. This leads to

Criterion 5 (Second-order stress test) *Given a placement, if for each admissible velocity \mathbf{v} there is a self stress $\boldsymbol{\omega}$ such that*

$$\Pi(\mathbf{v})\boldsymbol{\omega} \cdot \mathbf{v} > 0. \quad (35)$$

then the structure is stable in that placement.

A cleaner form of the above computation is given if we define the **stress operator**⁷

$$\Omega := \sum_{\text{edges}} \omega_{ij} B_{ij} \quad (36)$$

so that

$$\Pi(\mathbf{v})\boldsymbol{\omega} \cdot \mathbf{v} = \Omega \mathbf{v} \cdot \mathbf{v}. \quad (37)$$

A simple computation then gives the useful form for (35)

$$\Omega \mathbf{v} \cdot \mathbf{v} = \sum_{\text{edges}} \omega_{ij} (\mathbf{v}_i - \mathbf{v}_j)^2 > 0. \quad (38)$$

A physical motivation for this criterion is given by Calladine *et al.* (1991) [8]. If the admissible velocity \mathbf{v} is regarded as an infinitesimal perturbation of \mathfrak{p} , the perturbed geometric matrix is

$$\Pi(\mathfrak{p} + \mathbf{v}) = [\dots \boldsymbol{\pi}_{ij}(\mathfrak{p}) + \boldsymbol{\pi}_{ij}(\mathbf{v}) \dots] = \Pi(\mathfrak{p}) + \Pi(\mathbf{v}). \quad (39)$$

$\boldsymbol{\omega}$ is a prestress for \mathfrak{p} but not necessarily one for the placement $\mathfrak{p} + \mathbf{v}$. The force which would be required to maintain $\boldsymbol{\omega}$ in the new placement (the *geometric load vector*) would be

$$\mathfrak{f} = \Pi(\mathfrak{p} + \mathbf{v}) \boldsymbol{\omega} = \Pi(\mathbf{v}) \boldsymbol{\omega} = \sum \omega_{ij} B_{ij} \mathbf{v}, \quad (40)$$

and (35) then can be interpreted as

$$\mathfrak{f} \cdot \mathbf{v} > 0, \quad (41)$$

stating that *positive work must be done to move the structure from its original placement*, or, in other words, *the structure possesses first-order positive stiffness*.

⁷ This operator is the basis of the force density method. For a given stress vector $\boldsymbol{\omega}$, the self-equilibrium equation (7) becomes $\sum \omega_{ij} B_{ij} \mathfrak{p} = \Omega \mathfrak{p} = 0$ and can be regarded as a condition to be satisfied by the nodal coordinates. Due to the form of the operator B_{ij} , this condition is invariant under affine transformations of the nodal coordinates, Connelly *et al.* (1996) [10] (*cf* Williams (2003) [54]).

If the second-order stress test is not satisfied, we can pass to higher-order tests. The next few can be seen (*cf* Williams (2003) [54]) to be

$$\begin{aligned} & \sum \omega_{ij} B_{ij} \mathbf{q}_1 \cdot \mathbf{q}_2 > 0 \\ 2 \sum \omega_{ij} B_{ij} \mathbf{q}_1 \cdot \mathbf{q}_3 + \sum \omega_{ij} B_{ij} \mathbf{q}_2 \cdot \mathbf{q}_2 & > 0 \\ \sum \omega_{ij} B_{ij} \mathbf{q}_1 \cdot \mathbf{q}_4 + \sum \omega_{ij} B_{ij} \mathbf{q}_2 \cdot \mathbf{q}_3 & > 0, \end{aligned} \quad (42)$$

A final result, due to Roth *et al.* (1981) [39], is proved by different methods, *cf* Williams (2003) [54]. It says that when $\Pi(\mathfrak{p})$ satisfies the condition of maximal independence of column vectors, that is, when the evaluation at \mathfrak{p} produces a local maximum for the span of each subset of its column vectors (in their terms, when \mathfrak{p} is a *general placement*), the placement is stable if and only if it admits no admissible velocity. The argument is that under these conditions an admissible velocity always can be extended to a motion. We may refer to this as the **maximal-independence test**. Note, in particular, that the criterion is satisfied when the set of all column vectors is linearly independent.

3.3 Example

An instructive example is shown in Figure 3. In placement (a), if all edges are bars, the placement is stable and unstressed. To verify this, note that the geometric matrix is square:

$$\Pi(\mathbf{q}) = \begin{bmatrix} AC & AD & AB & BE \\ \mathbf{q}_A - \mathbf{q}_C & \mathbf{q}_A - \mathbf{q}_D & \mathbf{q}_A - \mathbf{q}_B & \mathbf{0} \\ \mathbf{0} & \mathbf{0} & \mathbf{q}_B - \mathbf{q}_A & \mathbf{q}_B - \mathbf{q}_E \end{bmatrix} \begin{matrix} A \\ B \end{matrix} \quad (43)$$

and, with the placement as illustrated, it is clear that the column vectors must be linearly independent, so the matrix is of full rank and admits neither self stress nor mechanism.

But, in the position shown, or any other in which no edges are collinear, if any of the edges is a cable, the structure is unstable. Physically, this is obvious; analytically, we note that since the placement admits no self stress, by the zero-self stress condition there is an admissible velocity which shortens the cable, and since the edge vectors are linearly independent, the maximal-independence test ensures that the structure is unstable.

If we adjust vertex B as in (b), rendering the edges AB and BE collinear, then the rank of the geometric matrix drops to three, so that both a self stress and a mechanism exist. The mechanism assigns velocity zero to node A , and a non-zero velocity, normal to the $AB - BE$ line, to node B . It is easy to see

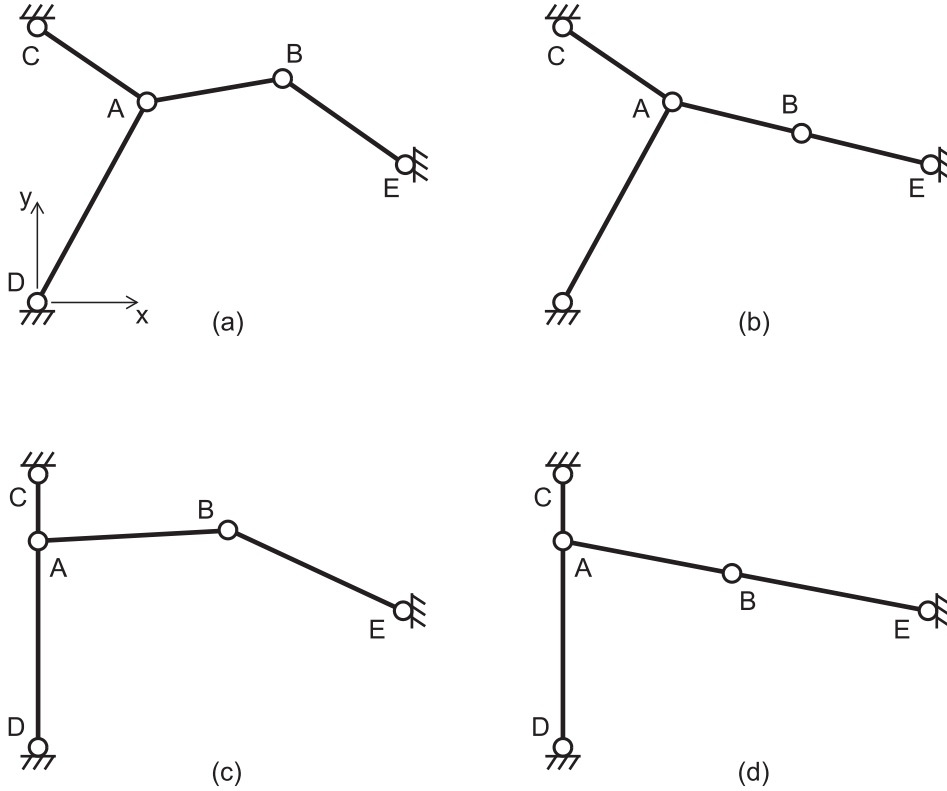


Fig. 3. A four-edge example

that all components of the self stress are of the same sign; we may choose them positive in order to use (35) to deduce stability. Any or all of the elements may be converted to cables and stability still is ensured.

Repositioning A as in placement (c), making AC and AD *vertical* and hence collinear, a different situation obtains, with only AC and AD stressable, regardless of the position of B . In this case there is a mechanism, moving both free nodes, but the stability analysis above still holds with AC and AD that can be converted to cables.

A final variation is placement (d), with AC and AD vertical and AB and BE collinear. In this placement, again we can stress only AC and AD . If AB and BE are bars, then the only *mechanism* affects only B , with motion of A occurring at the second order (zero velocity, non-zero acceleration). The interesting computation is that (38) now reveals the second-order stress test to fail. If we calculate the acceleration \mathfrak{o} as in (24) (with equality), it is easy to use the next test (42) to discover the stability of this placement. On the other hand, if either AB or BE is a cable, then there is another *admissible velocity*, which is not a mechanism: A can begin to move horizontally while the cable shortens. Again, one can calculate that the placement is stable in this case.

As noted earlier, the second-order test is not a necessary condition for stability,

as shown for placement (d), while it is necessary and sufficient for placements possessing first-order positive stiffness, like those in (b) and (c).

4 Sets of Stable Placements and the Rank-deficiency Manifold

As we have seen, stability of tensegrity structures is not insured in generic placements based on any simple rules of the number of edges and nodes and their connectivity (the *topology* of the structure). Thus there arises the problem of finding stable placements, if they exist, for a given topology. In this section we consider the structure of some collections of placements, emphasizing the distinction between bar structures and tensegrity structures. The characterizations are incomplete, but can serve for prescribing evolution of structures between stable placements. In particular, we focus on the rank-deficient manifold of classical tensegrity structures and describe differential equations which hold for paths on the manifold. The following section then details implementation of a numerical algorithm for solving these equations.

4.1 Case: if $\Pi(\mathbb{p})$ is of maximal rank

First, consider placements in which the $k \times 3n$ geometric matrix is over-square, *ie*, $k > 3n$ for three-dimensional structures ($k > 2n$ if 2-dimensional) and the rank is maximal. There are self stresses, but there can be no mechanisms. In this case the structure always is stable if it is a bar structure, but if it includes cables it may be unstable. (For example, consider the solid-line structure in Figure 3 (a) with an edge AE added, and one of AB or BE a cable.) However, if the placement admits a strict proper self stress then the structure is guaranteed to be rigid and hence is stable.

The set of maximal-rank placements, as the non-zero set of a determinant, is open, and within this set, the set with strict proper self stresses is open.

Next, suppose that $k \leq 3n$ (*alt* $2n$) and the matrix is of rank k . For a bar structure, there are two cases. If $k = 3n$, then there is no mechanism, and hence the structure is stable. If $k < 3n$ there is a mechanism and because the matrix is maximum rank this means the placement is unstable. For a tensegrity structure, in either case, the absence of a self stress ensures that there is an admissible velocity and since the rank is maximum it follows that the placement is unstable.

4.2 Case: if $\Pi(\mathfrak{p})$ is of sub-maximal rank. The rank-deficiency manifold

This is the more subtle and interesting case. Recall that m denotes the number of mechanisms and s the number of self stresses, so that

$$k - s = 3n - m. \quad (44)$$

For a given structure, consider placements in which the rank of Π is r . It is easy to see that the collection of all these placements form a smooth manifold⁸ in \mathbb{R}^{3n} and a little more difficult to show that at each point on the manifold the tangent plane consists in the vectors normal to

$$\mathfrak{n} := \sum \omega_{ij} B_{ij} \mathfrak{v} = \Pi(\mathfrak{v}) \boldsymbol{\omega} = \Omega \mathfrak{v} \quad (45)$$

for all choices of self stress $\boldsymbol{\omega}$ and mechanisms \mathfrak{v} at the point (Williams (2003) [54]). The set of all the normal vectors⁹ (45) span a subspace which we will denote as \mathbb{N} .

We consider a placement on the manifold at which *the second-order stress test holds*.

There are three subspaces of \mathbb{R}^{3n} of interest:

$$\mathbb{V} = \text{Null } \Pi(\mathfrak{p})^\top \quad \text{the subspace of mechanisms} \quad (46)$$

$$\mathbb{N} = \Omega(\mathfrak{p})\mathbb{V} \quad \text{the subspace of normal vectors} \quad (47)$$

$$\mathbb{P} := \text{Range } \Pi(\mathfrak{p}) = \text{Span } \{ \boldsymbol{\pi}_{ij}(\mathfrak{p}) \}. \quad (48)$$

Since the second-order test ensures that $\Omega \mathfrak{v} \cdot \mathfrak{v} \neq \mathbf{0}$ for all $\mathfrak{v} \in \mathbb{V}$, it follows that the null space of Ω does not intersect \mathbb{V} , so

$$\dim \mathbb{N} = \dim \mathbb{V} = 3n - \dim \mathbb{P}. \quad (49)$$

But the test also implies that \mathbb{N} and \mathbb{P} share only the zero vector since if $\mathfrak{n} = \Omega \mathfrak{v}$ were in both, we would have to have $\mathfrak{v} \cdot \Omega \mathfrak{v} = 0$. Hence \mathbb{N} and \mathbb{P} are complementary subspaces (although not orthogonal in general). It follows that the orthogonal projection of \mathbb{P} onto the tangent space of the manifold along \mathbb{N} is the entire tangent space.

Next, note that (12) and (13) imply that $2\boldsymbol{\pi}_{ij}$ is the gradient vector of $\boldsymbol{\lambda}_{ij}$. Our argument shows that when these edge vectors are projected onto the tangent space, they span that space. By assumption, they are linearly dependent; we may extract a linearly independent subset which will form a basis for the tangent space. This means that *the corresponding edge-lengths form a local*

⁸ As we verify below, it can happen that the manifold intersects itself.

⁹ Notice that this is the geometric load vector of (40).

coordinate system on the manifold. We will use this observation to prescribe paths traversing the manifold.

4.3 An example of self-intersection

Consider the structure in Figure 3. For a simple computation we set

$$\mathfrak{p}_D = (0, 0), \mathfrak{p}_C = (0, 2), \mathfrak{p}_E = (3, 1) \quad (50)$$

$$\mathfrak{p}_A = (x_A, y_A), \mathfrak{p}_B = (x_B, y_B) \quad (51)$$

The matrix Π is square, so that the rank-deficient placements are found from $\det \Pi = 0$, which becomes

$$x_A (x_B + x_A y_B - x_A - x_B y_A - 3y_B + 3y_A) = 0. \quad (52)$$

Thus $x_A = 0$ describes one manifold segment; it may be parameterized by y_A, x_B, y_B , while

$$y_B = (x_B y_A - x_B + x_A - 3y_A) / (x_A - 3) \quad (53)$$

is another, which can be parameterized by x_A, y_A, x_B . These two three-dimensional manifolds (in \mathbb{R}^4) meet in a two dimensional manifold and clearly are not parallel at the intersection. The placement at this intersection is that shown in Figure 3 (d); it can be parameterized by y_A and x_B .

At points on the 2-dimensional intersection manifold the normal vector calculation (45) yields only null vectors, but nonetheless it is possible to traverse through the point on one of the branches of the manifold since the normals continue smoothly on either side of the intersection.

4.4 Paths traversing the manifold

The only case which is simple to treat is that of *one mode of self stress* ($s=1$), so we consider only that case. We continue to assume that we have a placement \mathfrak{p} at which the second-order stress test is satisfied. Starting from this placement on the manifold, by the continuity of the null spaces, there is a neighborhood on the manifold where the second-order test is satisfied and $s = 1$, and hence the placements are stable. We consider how to construct paths on the manifold which stay within this neighborhood.

The first condition will ensure that the path $\mathfrak{q}(t)$ is on the manifold: we require

$$\dot{\mathfrak{q}} \cdot \mathfrak{n} = 0 \quad (54)$$

for each normal vector \mathfrak{n} at the placement $\mathfrak{q}(t)$. Recall that $\dot{\mathfrak{q}}$ represents the nodal velocities when we are moving from one placement to another while we use \mathfrak{v} to represent a mechanism in a given placement. The rate of change in each edge length as we move is

$$\boldsymbol{\pi}_{ij}(\mathfrak{q}(t)) \cdot \dot{\mathfrak{q}} = \epsilon_{ij}. \quad (55)$$

Since a selection of the edge-lengths serves as a coordinate system, we may vary those at will by choosing the appropriate ϵ_{ij} in (55). Then, adding condition (54) we obtain a system of $3n = \dim\mathbb{P} + \dim\mathbb{N}$ differential equations for $\mathfrak{q}(t)$, whose solution allows us to compute the other edge-lengths using (13). In the next section we detail this process.

Since

$$\sum \omega_{ij} \boldsymbol{\pi}_{ij}(\mathfrak{q}(t)) = 0, \quad (56)$$

using the stress vector at $\mathfrak{q}(t)$, we can take an inner product to see that

$$\sum \omega_{ij} \boldsymbol{\pi}_{ij} \cdot \dot{\mathfrak{q}} = 0, \quad (57)$$

which means that the edge-lengths obey

$$\sum \omega_{ij} \dot{\lambda}_{ij} = 2 \sum \omega_{ij} \epsilon_{ij} = 0. \quad (58)$$

This condition restricts the relative change of the edge-lengths at each point along the path¹⁰. It is identically satisfied if (54) holds.

5 The Marching Procedure

In this section we discuss the technique of creating a path along the rank-deficiency manifold in more detail. As before, we restrict ourselves to the case $k \leq 3n$ and $s = 1$ and assume that we are proceeding from a placement which satisfies the second-order stress test. The path on the manifold $\mathfrak{q}(t)$ is determined as the solution of the system of differential equations (54) and (55).

¹⁰ Recall that $\omega_{ij} = \tau_{ij}/\ell_{ij}$ and $\epsilon_{ij} = \ell_{ij} \dot{\ell}_{ij}$, with ℓ_{ij} being the length of the edge ij . Therefore, this condition takes the form $\sum \tau_{ij} \dot{\ell}_{ij} = 0$, meaning that the internal forces spend null power on the path. Since the self stress vector also represents the vector of *incompatible lengthenings* (Pellegrino *et al.* (1986) [36]), *ie*, those which do not preserve the connectivity of the structure, (58) can be seen as the orthogonality condition between $\boldsymbol{\epsilon}$ and the incompatible lengthenings.

5.1 The system of equations

Since the dimension of the subspace of self stresses is one, we write $\dim \mathbb{P} = (k - 1)$ equations, assigning a lengthening-rate to $(k - 1)$ edge vectors. By the complementarity of \mathbb{N} and \mathbb{P} , we can complete the differential system with the normal conditions between $\dot{\mathbf{q}}$ and the $(3n - k + 1) = \dim \mathbb{N}$ independent normal vectors.

The simplest marching process involves changing the length of only two edges, say ab and cd . To move away from the starting placement, we change the length of ab at a designated rate ϵ_{ab} . For a generic edge $hk \neq ab, cd$ the lengthening-rate is set equal to zero. For this process, we solve

$$\begin{cases} \boldsymbol{\pi}_{ab} \cdot \dot{\mathbf{q}} = \epsilon_{ab} \\ \boldsymbol{\pi}_{hk} \cdot \dot{\mathbf{q}} = 0 & \forall hk \neq ab, cd \\ \mathbf{n} \cdot \dot{\mathbf{q}} = 0 & \forall \mathbf{n} \in \mathbb{N} \end{cases} \quad (59)$$

for $\mathbf{q}(t)$ and then calculate the change in length of the other chosen edge, cd .

As an example, let us consider the solid-line placement in Figure 4 for which we change the lengths of AB and CD , with $\epsilon_{AB} < 0$. The lengthening of AD is determined through the solution of the following system

$$\begin{cases} \boldsymbol{\pi}_{AB} \cdot \dot{\mathbf{q}} = \epsilon_{AB} \\ \boldsymbol{\pi}_{AC} \cdot \dot{\mathbf{q}} = 0 \\ \boldsymbol{\pi}_{BE} \cdot \dot{\mathbf{q}} = 0 \\ \mathbf{n} \cdot \dot{\mathbf{q}} = 0 \end{cases} \quad (60)$$

With these settings the nodes A and B follow the thin solid-line circular trajectories; the normal condition ensures that AB and BE remain collinear and AD is lengthened accordingly, as shown by the dotted-line placement.

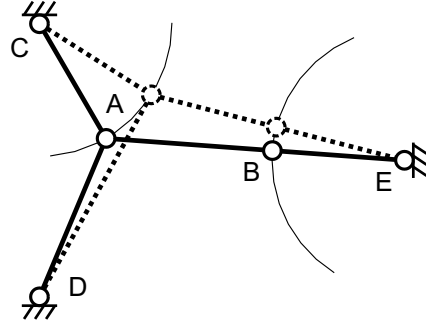


Fig. 4. Moving from one placement to another.

Often it is desirable to change the lengths of many edges at the same time, for example to preserve some symmetry. In such a case, we might choose two disjoint subsets $\mathcal{E}_1, \mathcal{E}_2$, of k_1, k_2 edges respectively, and assign the same lengthening-rate, ϵ_1, ϵ_2 , respectively, to each edge in each group. In this case

we have the system

$$\begin{cases} \boldsymbol{\pi}_{ij} \cdot \dot{\mathbf{q}} = \epsilon_1 & \forall ij \in \mathcal{E}_1 \\ \boldsymbol{\pi}_{hk} \cdot \dot{\mathbf{q}} = 0 & \forall hk \in \mathcal{E} \setminus \{\mathcal{E}_1 \cup \mathcal{E}_2\} \\ (\boldsymbol{\pi}_{fg} - \boldsymbol{\pi}_{lm}) \cdot \dot{\mathbf{q}} = 0 & \forall fg, lm \in \mathcal{E}_2 \\ \mathfrak{n} \cdot \dot{\mathbf{q}} = 0 & \forall \mathfrak{n} \in \mathbb{N} \end{cases} \quad (61)$$

The unknown lengthening ϵ_2 is then obtained from the solution of this system.

Analogously, for general cases, we can choose different lengthening-rates, possibly changing with time, within each subset \mathcal{E}_1 and \mathcal{E}_2 , setting those in \mathcal{E}_1 directly, and those in \mathcal{E}_2 to be proportional to an assigned vector $\boldsymbol{\epsilon}_2 = \alpha \bar{\boldsymbol{\epsilon}}$. Thus we write for these edges the $(k_2 - 1)$ independent equations of the form

$$\left(\boldsymbol{\pi}_{fg} - \frac{\bar{\epsilon}_{fg}}{\bar{\epsilon}_{lm}} \boldsymbol{\pi}_{lm} \right) \cdot \dot{\mathbf{q}} = 0. \quad (62)$$

As before, the unknown parameter α is obtained from the solution of the differential system.

5.2 Limiting placements

Next, we consider possible difficulties arising when one deals with the differential system (59), choosing to vary only two lengths.

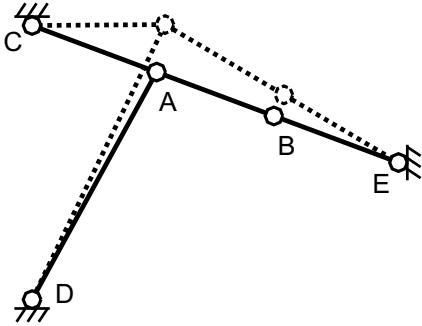


Fig. 5. Moving from a limit placement.

In the previous example in Figure 4 it is not possible to shorten AB indefinitely, because its length can reach a minimum value. This value corresponds to the **limit placement** represented by the solid-line in Figure 5, where the three edges AC , AB and BE are collinear. It is easy to see that this limit placement occurs at a smooth point of the rank-3 manifold, so this does not represent a break in the manifold.

Moreover, starting from the limit placement and lengthening the edge AB , there exist two possible paths on the manifold, advancing toward either the dotted-line placement in Figure 4 or that in Figure 5. The important fact is that the edge AD is unstressed in the limiting placement. Calling the subsystem composed of all *stressed* edges a **minimal subsystem**, we discover that

we cannot arbitrarily assign the lengthenings of all edges belonging to such a subsystem. Indeed, from (57), or (58), we have

$$0 = \omega_{AD} \boldsymbol{\pi}_{AD} \cdot \dot{\mathbf{q}} + \omega_{AB} \boldsymbol{\pi}_{AB} \cdot \dot{\mathbf{q}} = \omega_{AD} \epsilon_{AD} + \omega_{AB} \epsilon_{AB}, \quad (63)$$

since the edges AC and BE do not change in length. This relation shows that, since in the limit placement $\omega_{AD} = 0$ and $\omega_{AB} \neq 0$, the lengthening of AB must be zero. This example illustrates the role that stresses play while moving along the rank-deficiency manifold. *When the edges that change their lengths have stresses of the same sign, one edge shortens and the other lengthens* (Figure 4); *when the stresses are of opposite sign, they both lengthen or shorten* (Figure 5).

As a second example, consider the structure in Figure 6. We assign a positive lengthening to AD and zero lengthening to AB and BE , while the lengthening of AC is to be determined. The normal condition requires that AC and AD remain aligned. Following these rules we arrive at the dotted-line limit placement: AD cannot be further lengthened since AB and BE are aligned. In this case, both ω_{AB} and ω_{BE} are zero throughout the process.

This is a different type of limit placement in that, as noted earlier, it belongs to the intersection of two rank-deficiency manifolds. The tangent space is undefined on this intersection and the computation of the normal vector gives a null vector as a result. Progress from this placement requires a commitment to one branch or the other of the manifold, and the corresponding normals must be selected as the limit of those from adjacent placements.

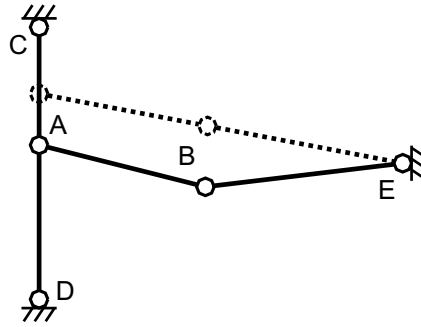


Fig. 6. Another limit placement.

5.3 Implementation in MATLAB

The MATLAB programming package has been employed for numerical computations, for both the stability analysis and the marching process.

Figure 7 shows the flow-chart that summarizes our analysis on a given system. In the first step the collection of nodes and edges is assigned, some of the nodes being constrained to fixed locations. Here n represents the number of free nodes but the vector \mathbf{p} contains all (free and fixed) nodal coordinates, so that any vector representing velocities or higher order derivatives contains zeros as

fixed entries. In the second step we construct the matrix $\Pi(\cdot)$ as a function that can be evaluated at any nodal placement. Next (step 3), the rank of the geometric matrix $\Pi(\mathfrak{p})$ is computed; this gives also the dimensions s and m of the nullspaces of self stresses and mechanisms. With this information we can pass through tests from step 4 to step 7 to identify the system type. In the case of a full-rank geometric matrix (tests 4 – 6), we have the following cases: for a square matrix, the system is stable if and only if there are no cables; for $s > 0$, the system is stable if and only if there is a positive self stress in all cables; for $m > 0$ the system is unstable. The last test checks for a submaximal rank with $s = 1$; this is to exclude more complicated situations, whose methodology of analysis will be outlined in a following paper. In the eighth step we compute the quantity $\Omega \mathfrak{v} \cdot \mathfrak{v}$ from the self stress and the mechanisms of the system and, in the ninth step, perform the second-order test to be ready for the marching process. To this end, it is sufficient to test the positivity of a reduced matrix $\hat{\Omega}$ whose (h, k) entry is the scalar product of the h -th independent normal vector with the k -th independent mechanism. If the test fails, then (step 10), if $\hat{\Omega}$ is positive semidefinite we need a higher-order analysis, otherwise the system is definitely unstable. We now can choose the two subsets of edges \mathcal{E}_1 and \mathcal{E}_2 in step 11 and assign their lengthenings (step 12). In step 13 we check that the chosen set of prescribed lengthenings if $\mathcal{E} \setminus \mathcal{E}_2$ is not a minimal subsystem, otherwise we need to modify our choice in step 11. Finally, in step 14 the differential system is solved. Recall that the stability of the placements on the resulting path is ensured only in a neighborhood of the starting placement, hence, for sufficiently small changes of the length of the elements.

The MATLAB built-in function ‘*ode45*’ is suitable to solve the differential system numerically. This function employs the Runge-Kutta method and solves systems of the form $\mathbf{M}(\mathfrak{q}, t)\dot{\mathfrak{q}} = \mathbf{f}(\mathfrak{q}, t)$ where \mathbf{M} is the so-called mass matrix and \mathbf{f} is the vector of known terms. According to (61) and (62), here the rows of \mathbf{M} are the edge vectors, the linear combinations of them and the normal vectors; the entries of \mathbf{f} are the corresponding lengthenings and zeros.

In step 3 and during step 14, the rank of the geometric matrix and the associated nullspaces are computed using the singular value decomposition (see Pellegrino (1993) [38]), through the MATLAB function ‘*svd*’. This function gives the sets of singular vectors and the (positive) singular values in decreasing order. The singular values that are close to zero correspond to the co-rank ($\min\{3n, k\} - r$) of the geometric matrix; the singular values then represent a measure of how close the placement is to the rank-deficiency manifold. For analytically determined rank-deficient placements, these values are of the order of 10^{-14} or lower. During the resolution of the differential system ($s = 1$) the unique value close to zero may grow but it is found that the ratio with the previous one remains at least of the order 10^{-3} . Usually this ratio grows excessively when the marching process requires the system to pass through a limit placement.

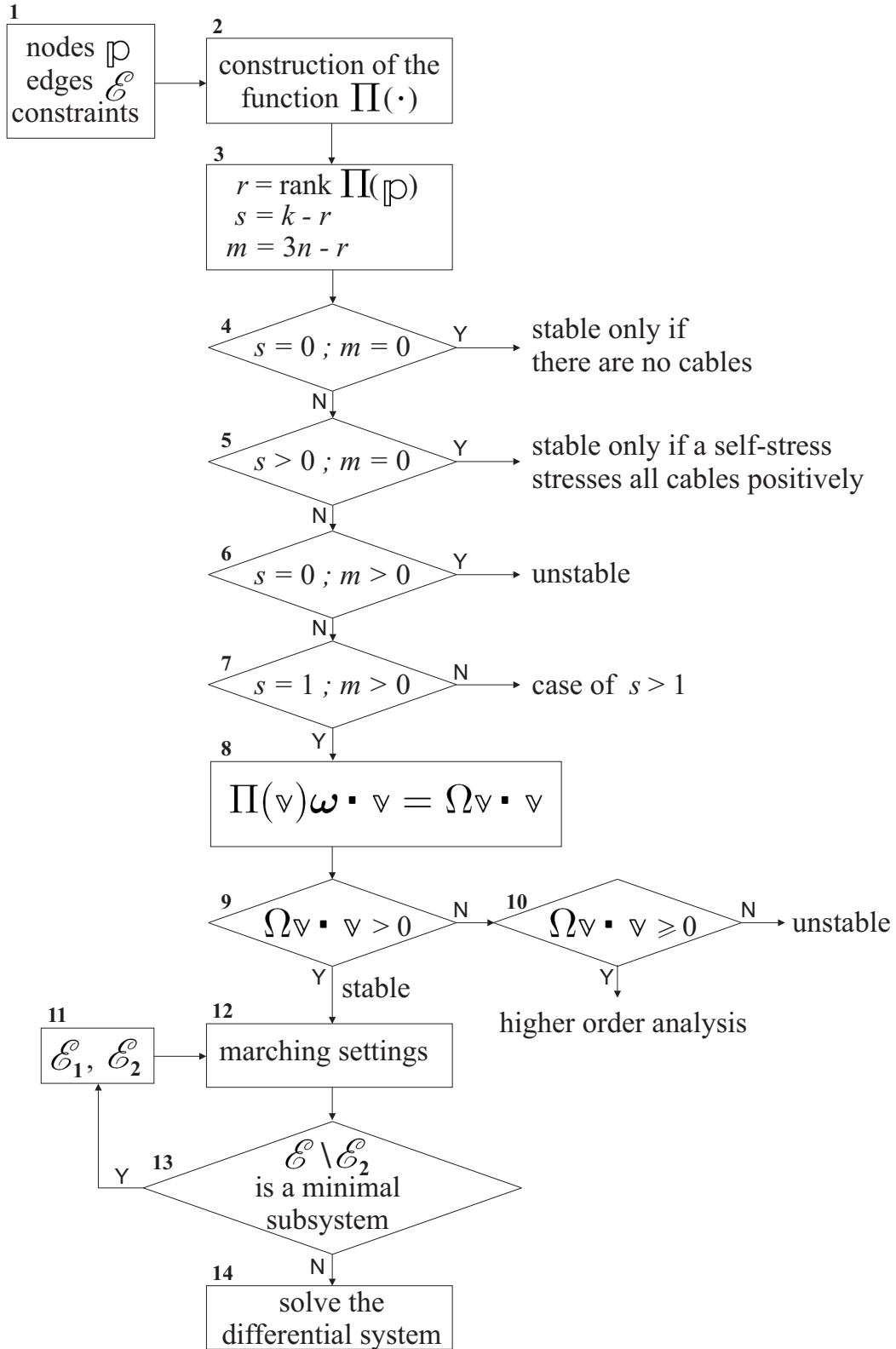


Fig. 7. Flowchart for the algorithm.

5.4 Numerical computations

We present some results for the example of Figure 3. The coordinates of constrained nodes are given as in Section 4.3; edges AC and BE have fixed length equal to $\sqrt{2}$ and 1 respectively. Figure 8 shows four different placements; we

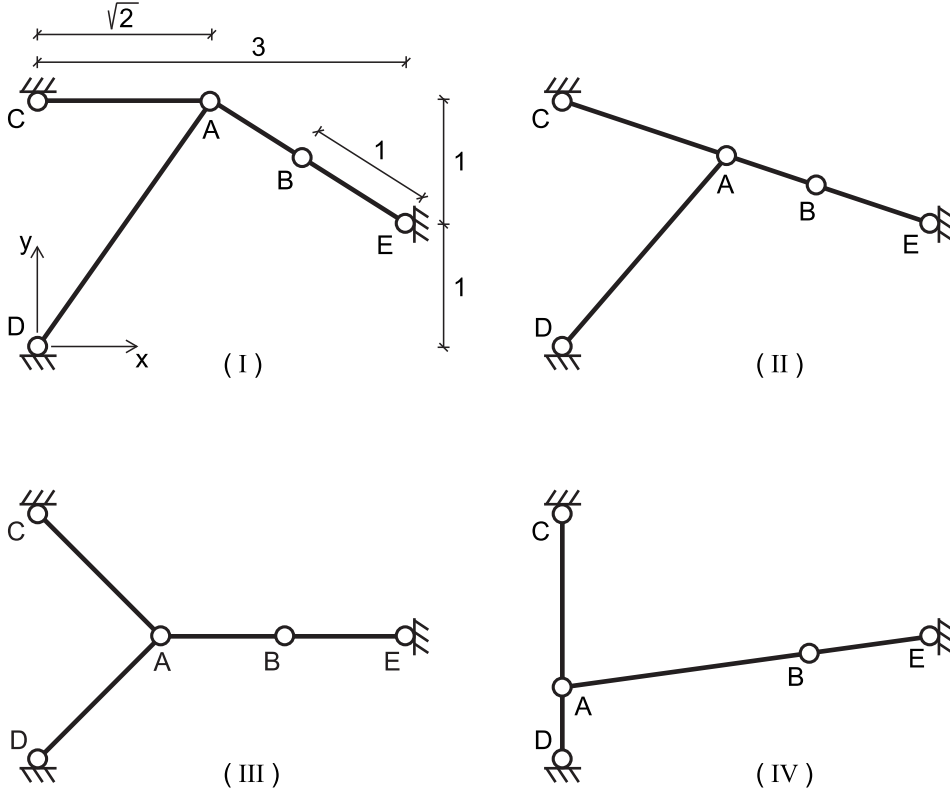


Fig. 8. Sample calculations

pass from one to another of these placements by changing the lengths of AD and AB . The last placement lies on the self-intersection of the manifold, while the other three belong to the part of the manifold represented by equation (53). In particular, in the first position (I) the edge AC is horizontal; the second position (II) correspond to the first kind of limit placement discussed in 5.1; in the third position (III) edges AB and BE are aligned horizontally. Edges AC and BE are fixed in length and their corresponding independent lengthening are zero. The last independent lengthening can be assigned to AD or AB by using the relation

$$\epsilon_{ij}\Delta t = \frac{1}{2}(\ell_{ij,fin}^2 - \ell_{ij,in}^2), \quad (64)$$

obtained by integrating the equation $\dot{\ell}_{ij} = \text{const} = \epsilon_{ij}$ and relating the initial and final length of an element with its lengthening during an interval of time. For processes starting from (or passing through) position II, we are forced to

Initial-final placement	Independent non-null lengthening	Maximum error on final coordinates $\Delta x_P = x_{P,num} - x_{P,an}$	Singular values ratio
I-II	$\epsilon_{AB} < 0$	$ \Delta y_A \simeq 3 \cdot 10^{-3}$	10^{-10}
I-II	$\epsilon_{AD} < 0$	$ \Delta x_B \simeq 4 \cdot 10^{-12}$	10^{-12}
I-III	$\epsilon_{AD} < 0$	$ \Delta y_B \simeq 3 \cdot 10^{-9}$	10^{-10}
III-I	$\epsilon_{AD} > 0$	$ \Delta x_B \simeq 10^{-9}$	10^{-9}
II-III	$\epsilon_{AD} < 0$	$ \Delta x_A \simeq 2 \cdot 10^{-10}$	10^{-11}
III-II	$\epsilon_{AB} < 0$	$ \Delta y_A \simeq 3 \cdot 10^{-3}$	10^{-9}
III-II	$\epsilon_{AD} > 0$	$ \Delta x_A \simeq 4 \cdot 10^{-11}$	10^{-11}
I-IV	$\epsilon_{AD} < 0$	$ \Delta x_A \simeq 2 \cdot 10^{-3}$	10^{-8}
II-IV	$\epsilon_{AD} < 0$	$ \Delta x_A \simeq 2 \cdot 10^{-3}$	10^{-8}
III-IV	$\epsilon_{AD} < 0$	$ \Delta x_A \simeq 10^{-3}$	10^{-10}
III-IV	$\epsilon_{AB} > 0$	$ \Delta y_B \simeq 5 \cdot 10^{-3}$	10^{-7}

Table 1
Numerical results.

assign the lengthening of AD , because we cannot fix all the lengthenings of the minimal subsystem $\{AC, AB, BE\}$. We remember that if we want to start a process from placement IV we need to provide the initial normal vector.

Table 1 shows some results for different marching processes between the placements; the result are obtained by the MATLAB solver with default settings. For each process we report the maximum difference between analytically and numerically computed final nodal coordinates. We report also the order of the ratio between the last two singular values of the geometric matrix in the final placement; this ratio is of the order of 10^{-17} at the beginning of each process. If the final placement is the limit placement II (processes I-II and III-II), when the independent lengthening is that of AB , then the error on the coordinates may grow up to 10^{-3} : the limiting placement cannot be reached precisely since the independent length reaches a minimum value. This is also the case of processes that end in the limit placement IV with independent lengthening of AD . The last case III-IV with independent lengthening of AB gives worse results, this is due to the non-existence of the normal vector in placement IV.

We end by showing an application of the method to a large three-dimensional structure. We applied the marching procedure to a tensegrity tower, the kind of decorative structure often realized by Snelson. Figure 9 shows an arch-shaped structure obtained from the tower by lengthening (shortening) the cables on

the upper (lower) side of the arch. A simplified analytical solution for the form-finding problem of this kind of towers is given in Micheletti (2003) [24] and it is used to construct the starting placement. For the tower in question, the ratio between the last two singular values is of the order of 10^{-14} . The choice of the edge lengthenings ϵ_{ij} is crucial in order to avoid limiting placements; in some cases we reached the arch-shaped placement but we found this ratio to grow excessively, up to 10^{-2} , and the self stress to take values close to zero in most of the elements. For a careful choice of the process, this ratio can be of the order of 10^{-5} or lower at the final placement; the self stress results then are uniform along the arch and non-zero in each edge.

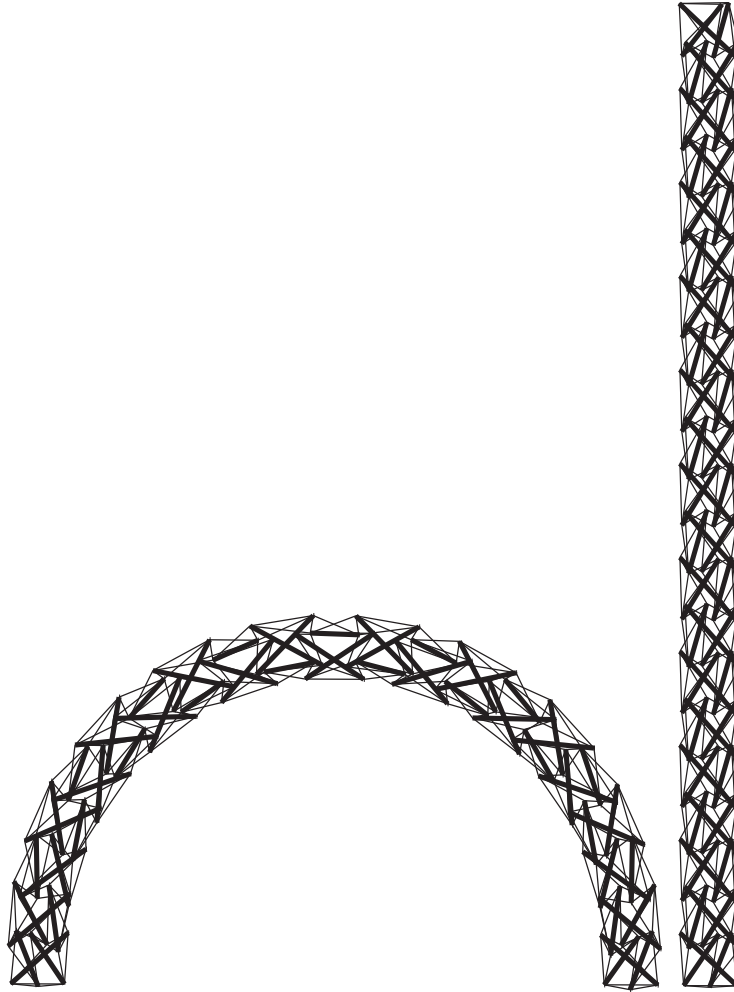


Fig. 9. The algorithm was used to convert the tower to the arch.

6 Discussion

We presented a method for finding one-parameter families of stable placements for tensegrity structures, starting from a known initial stable placement. The method applies to the set of rank-deficient placements which is characterized within a general classification of tensegrity structures. This classification is obtained from an ordered collection of known results which were previously scattered through the mathematical and engineering literature.

After having discussed the case of a full-rank geometric matrix, we have given the characterization of the rank-deficiency manifold through the identification of its normal (45). We proved that a subset of the edge-lengths can be chosen as a local coordinate system on the manifold, Then we have focused on the simple case of a single state of self stress. The kinematic equations (55) relating the nodal velocities $\dot{\mathbf{q}}$ to the lengthenings ϵ_{ij} of the chosen coordinate system have been used to prescribe a path on the manifold, together with the prescription (54), that the nodal velocities must belong to its tangent space. The resulting differential system has been implemented and solved by using the routines available in MATLAB.

The characterization of the manifold is a key feature of the method. It appears to be not known in the literature while some of the existing form-finding methods might benefit of its application. A main advantage, with respect to other approaches, is that the lengths of the elements are directly controlled. This feature makes the method well suited for the rapid analysis of variable geometry structures, such as deployable or tendon controlled systems.

The method can be applied reliably to large structures, in general with multiple mechanisms ($m \geq 1$). The last $(m + 1)$ singular values of the geometric matrix serve to measure the accuracy of the placements on the manifold. The accuracy decays as a limit placement is approached.

Condition (58) gives insight to the marching process. It not only establishes the relation between the signs of stresses and lengthenings during a process but also justifies the definition of limit placement and minimal subsystem.

We have shown that the final placement is stable in a neighborhood of a starting stable placement, however in the simulations it is possible to reach stable placements which are very far from the initial one. For complicated cases, it can be necessary to test for stability each point of the path to avoid the occurrence of unstable portions.

We remark again that our model considers only rigid bars and inextensible cables connected by pin-joints, so that the material properties of the elements

in a corresponding physical structure are not necessary for the form-finding process. On the other hand, local or global buckling instabilities, which depend on the material employed, on the magnitude of the self stress and on magnitude of the external loads, have to be considered separately. However, the stability of a physical realization of a structure satisfying the second-order stress test can still be ensured by limiting the magnitude of the self stress and/or of the external loads. Regarding the problem of cable-slackening, it is important to avoid placements with an high ratio between the stress in bars and cables.

Concerning future improvements, some aspects are important which are not covered in this paper. A first and straightforward improvement consists in including geometry constraints. They can be easily written in the form $\mathbf{c} \cdot \dot{\mathbf{q}} = 0$, with \mathbf{c} a constant or time dependent vector characterizing the constraint. A second and more difficult task would be the extension of the method to include stress control of some edges. Lastly, a necessary step for forthcoming studies is the development of a procedure in case of multiple states of self stress. In regard to this, we remark that the characterization of the rank-deficiency manifold still holds but the details of such a procedure remain to be outlined.

7 Conclusions

The proposed procedure represents a new and simpler approach for discovering the range of geometries that are feasible for a given topology of a tensegrity structure. It applies to the set of rank-deficient placements and it needs the knowledge of an initial stable placement. The method is independent of the material properties of the structures. It is important for the development of variable geometry applications since it employs the edge-lengths as control parameters for moving on a continuous path of stable placements. The characterization of the rank-deficiency manifold, together with the collection of previous results, allow for more insight in the form-finding process comparing to existing approaches. The method can be applied to large structures with accurate results and it can be extended to the more complicate case of multiple states of self stress.

Acknowledgements

The research presented in this paper has been partly conducted during AM's visit to the Department of Mathematical Sciences of Carnegie Mellon University, during the year 2004. Financial support from the Center of Nonlinear Analysis is gratefully acknowledged.

We would also like to acknowledge several useful suggestions from the reviewers.

References

- [1] J. B. Aldrich, R. E. Skelton, K. Kreutz-Delgado, “Control synthesis for a class of light and agile robotic tensegrity structures”, in *Proceedings of the IEEE American Control Conference*, Denver, Colorado (2003).
- [2] V. Alexandrov, “Implicit function theorem for systems of polynomial equations with vanishing jacobian and its application to flexible polyhedra and frameworks”, *Monatshafte fur Math.* **132** (2001), 269–288.
- [3] L. Asimow, B. Roth, “The rigidity of graphs II”, *J. Math. Anal. Appl.* **68** (1979), 171–190.
- [4] M. Bouderbala, R. Motro, “Folding tensegrity systems”, in *Proceedings of IUTAM/IASS Symposium on Deployable Structures: Theory and Applications*, Cambridge, U.K. (1998).
- [5] M. R. Barnes, “Form finding and analysis of tension structures by dynamic relaxation”, *Int. J. Space Struct.* **14**:2 (1999), 89–104.
- [6] R. W. Burkhardt, “A practical guide to tensegrity design” 2nd edition, Cambridge, Massachusetts: Tensegrity Solutions (2005).
- [7] C. R. Calladine, “Buckminster Fuller’s ‘tensegrity’ structures and Clerk Maxwell’s rules for the construction of stiff frames”, *Int. J. Solids Struct.* **14** (1978), 161–172.
- [8] C. R. Calladine, S. Pellegrino, “First-order infinitesimal mechanisms”, *Int. J. Solids Struct.* **27** (1991), 505–515.
- [9] A. L. Cauchy, “Sur les polygones et le polyhédres”, *XVIIe Cahier* **9** (1813), 87–89.
- [10] R. Connelly, W. Whiteley, “Second-order rigidity and prestress stability for tensegrity frameworks”, *SIAM J. Discrete Math.* **9** (1996), 453–491.
- [11] R. Connelly, A. Back, “Mathematics and tensegrity”, *American Scientist* **86**:2 (1998), 142–151.
- [12] A. S. Day, “An introduction to dynamic relaxation”, *The Engineer* **219** (1965), 218–221.
- [13] M. Defosse, “Shape memory effect in tensegrity structures”, *Mechanics Research Communications*, **30** (2003), 311–316.
- [14] A. El Smaili, R. Motro, V. Raducanu, “New concept for deployable tensegrity systems, structural mechanics activated by shear force”, in *Proceedings of IASS04, Int. Association for Shell and Spatial Structures*, Montpellier, France (2004), 318–319.
- [15] E. Fest, K. Shea, I. F. C. Smith, “Active Tensegrity Structure” *Journal of Structural Engineering* **130**:10 (2004), 1454–1465.

- [16] H. Furuya, “Concept of deployable tensegrity structures in space applications”, *Int. J. Space Structures* **7:2** (1992), 143–151.
- [17] H. Glück, “Almost all simply connected surfaces are rigid”, in Geometric Topology, *Lecture Notes in Math* **438**, Springer Verlag (1975), 225–239.
- [18] G. Gomez Estrada, H. J. Bungartz, C. Mohrdieck “Numerical form-finding of tensegrity structures”, *Int. J. Solids Struct.*, in press (2006).
- [19] A. Hanaor, “Double-layer tensegrity grids as deployable structures”, *Int. J. Space Struct.* **8:1–2** (1993), 135–143.
- [20] W. T. Koiter, “On Tarnai’s conjecture with reference to both statically and kinematically indeterminate structures”, Tech. Rep. 788, Laboratory for Engineering Mechanics, Delft, The Netherlands (1984).
- [21] K. Linkwitz, H. J. Schek, “Einige bemerkungen zur berechnung von vorgespanten seilnetzkonstruktionen”, *Ingenieur-Archiv* **40** (1971), 145–158.
- [22] M. Masic, R. E. Skelton, P. E. Gill, “Optimization of tensegrity structures”, *Int. J. Solids Struct.* **43** (2006), 4687-4703.
- [23] J. C. Maxwell, “On reciprocal diagrams, frames and diagrams of forces”, *Trans. Roy. Soc. Edinburgh* **26** (1869), 1–40.
- [24] A. Micheletti, “The indeterminacy condition for tensegrity towers, a kinematic approach”, *Rev. Fr. de Génie Civil* **7** (2003), 329–342.
- [25] A. Micheletti, W. O. Williams, “A marching Procedure for form-finding for tensegrity structures”, accepted for publication, *J. Mech. Material Struct.*
- [26] A. F. Möbius, “Lehrbuch der statik vol 2”, Göschen, 1837.
- [27] R. Motro, “Forms and forces in tensegrity systems”, in *Proceedings of 3rd International Conference on Space Structures*, Amsterdam, The Netherlands (1984), 180–185.
- [28] R. Motro, “Tensegrity: structural systems for the future”, London, U.K.: Kogan Page Science (2003).
- [29] H. Murakami, Y. Nishimura, “Static and dynamic characterization of regular truncated icosahedral and dodecahedral tensegrity modules”. *Int. J. Solids Struct.* **38:50/51** (2001), 9359–9381.
- [30] Y. Nishimura, “Static and dynamic analyses of tensegrity structures”, Ph.D. dissertation, University of California at San Diego, La Jolla, California (2000).
- [31] M. Ohsaki, J. Y. Zhang, “Stability conditions of prestressed pin-jointed structures”, *Int. J. Non-Linear Mechanics*, submitted (2005).
- [32] I. J. Oppenheim, W. O. Williams, “Tensegrity prisms as adaptive structures”, *Adaptive Structures and Material Systems ASME* **54** (1997), 113-120.

- [33] C. Paul, H. Lipson, F. J. Valero Cuevas, “Evolutionary form-finding of tensegrity structures”, in *Proceedings of the 2005 Genetic and Evolutionary Computation Conference*, Washington D.C. (2005).
- [34] C. Paul, H. Lipson, F. J. Valero Cuevas, “Design and control of tensegrity robots for locomotion”, *IEEE Transactions on Robotics*, accepted (2005).
- [35] S. Pellegrino, “Mechanics of kinematically indeterminate structures”, Ph.D. dissertation, University of Cambridge, U.K. (1986).
- [36] S. Pellegrino, C. R. Calladine, “Matrix analysis of statically and kinematically indeterminate frameworks”, *Int. J. Solid Struct.* **22** (1986), 409–428.
- [37] S. Pellegrino, “A class of tensegrity domes”, *Int. J. Space Struct.* **7** (1992), 127–142.
- [38] S. Pellegrino, “Structural computations with the singular value decomposition of the equilibrium matrix”, *Int. J. Solids Struct.* **30** (1993), 3025–3035.
- [39] B. Roth, W. Whiteley, “Tensegrity frameworks”, *Trans. Am. Math. Soc.* **265** (1981), 419–446.
- [40] G. Salerno, “How to recognize the order of infinitesimal mechanisms: A numerical approach”, *Int. J. Num. Meth. Eng.* **35** (1992), 1351–1395.
- [41] H. J. Schek, “The force density method for form finding and computation of general networks”, *Computer Methods in Applied Mechanics and Engineering* **3** (1974), 115–134.
- [42] M. Schenk, J. L. Herder, S. D. Guest, “Design of a statically balanced tensegrity mechanism”, in *Proceeding of IDECT/CIE 2006 ASME 2006 International Design Engineering Technical Conferences & Computers and Information in Engineering Conference*, Philadelphia, Pennsylvania (2006).
- [43] K. D. Snelson, “Snelson on the tensegrity invention”, *Int. J. Space Struct.* **11** (1996), 43–48.
- [44] R. E. Skelton, J. W. Helton, R. Adhikari, J. P. Pinaud, W. Chan, “An introduction to the mechanics of tensegrity structures”, in *The Mechanical Systems Design Handbook: Modeling, Measurement and Control*, London, U.K.: CRC press (2001).
- [45] R. E. Skelton, D. Williamson, J. Han, “Equilibrium conditions of a class I tensegrity structure”, in *Spaceflight Mechanics, Advances in the Astronautical Sciences*, **112:2** (2002), 927-950.
- [46] A. M. So, Y. Ye, “A semidefinite programming approach to tensegrity theory and realizability of graphs”, in *Proceedings of the 17th Annual ACM-SIAM Symposium on Discrete Algorithms*, Miami, Florida (2006).
- [47] C. Sultan, R. E. Skelton, “Tendon control deployment of tensegrity Structures”, in *Proceeding of SPIE, 5th International Symposium on Smart Structures and Materials*, San Diego, California (1998).

- [48] C. Sultan, M. Corless, R. E. Skelton, “The prestressability problem of tensegrity structures. Some analytic solutions”, *Int. J. Solids Struct.* **38** (2001), 5223-5252.
- [49] T. Tarnai, “Comments on Koiter’s classification of infinitesimal mechanisms”, Tech. rep., Hung. Inst. Build. Sci., Budapest, Hungary (1984).
- [50] A. G. Tibert, “Deployable tensegrity structures for space applications”, Ph.D. dissertation, Royal Institute of Technology, Stockholm, Sweden (2002).
- [51] A. G. Tibert, S. Pellegrino, “Review of form-finding methods for tensegrity structures”, *Int. J. Space Struct.* **18**:4 (2003), 209–223.
- [52] N. Vassart, R. Motro, “Multiparametered formfinding method: application to tensegrity systems”, *Int. J. Space Struct.*, **14**:2 (1999), 147–154.
- [53] N. Vassart, R. Laporte, R. Motro, “Determination of mechanism’s order for kinematically and statically indetermined systems”, *Int. J. Solids Struct.* **37** (2000), 3807–3839.
- [54] W. O. Williams, “A primer on the mechanics of tensegrity structures”, Tech. rep., Center for Nonlinear Analysis, Department of Mathematical Sciences, Carnegie Mellon University, Pittsburgh, Pennsylvania (2003).
- [55] J. Y. Zhang, M. Ohsaki, “Form-finding of self-stressed structures by an extended force density method”, in *Proceedings of IASS05, Int. Association for Shell and Spatial Structures*, Bucharest, Romania (2005), 93–110.
- [56] L. Zhang, B. Maurin, R. Motro, “Form-finding of nonregular tensegrity systems”, *J. Structural Engineering* **132**:9 (2006), 1435–1440.